Shelf Life Prediction of Post-Harvested Pomegranate using Enhanced Deep Learning

Surekha V Yakatpure[1*]

Department of ECE
Visveswaraya Technical University, Belagavi, Karnataka
[*]Email: surekha.sakhare@gmail.com

Dr. Krupa R Rasane[2]

Professor & Head,
Department of Electronics and Communication,
Jain College of Engineering Belgavi, Karnataka-590014, India.
Email: kru_ran@yahoo.com

Dr. K. Dinesh Babu[3]

Principal Scientist,
National Research Centre on Pomegranate (NRCP),
Solapur, Maharashtra- 413255, India.
Email: ckdhinesh@gmail.com

Abstract

One of the major requirements of agriculture is the quality assessment and ripeness of the agricultural products using non-destructive techniques. The ability of deep learning (DL) models to accurate classification and prediction are increasing. The work's major aim is to use the DL model to predict the shelf life of pomegranate fruits. Initially, the input MRI pomegranate images are resized to the proper size. Then, the features are extracted and classified using the deep learning model (DL) S-ResNet-152 (Squeeze based ResNet-152). This DL model classifies fruits as healthy or unhealthy. Further, for optimizing the layers and minimizing the loss function, the metaheuristic optimization improved sandpiper optimization (ISO). Then, the healthy fruits are considered for the prediction process. Here, the pomegranate fruit's shelf life is predicted using the DL model. The features like physiochemical and physiological loss in weight (PLW) and Firmness are predicted for determining the fruit quality. These features are given as input to the hybrid DL model bidirectional gated auto network (Bi-GRU-AN) is used for the prediction of shelf life. The performance of the proposed classification and prediction results are compared with other DL models in terms of the square of correlation coefficient (R^2), root mean square error of calibration (RMSEC), and root mean square error of validation (RMSEV).

Keywords: **Classification; prediction; pomegranate fruits; metaheuristic optimization; shelf life; deep learning model.**

1. Introduction

Pomegranate (Punica granatum) is very popular, and it is highly grown in tropical and subtropical regions from the family punicaceae. It is more common and highly grown in Mediterranean regions, India, China, Egypt, France, Japan, USA etc. [Felicia *et al.* (2022)] [Özdemir and Gökmen (2017); Dak *et al.* (2014)]. Nearly 1 million tons of annual production is produced in leading countries like India, the middle east etc. It also has the leading demand in producing fresh juice, syrup, wine, candy, etc. [Althaus and Blanke (2021)]. With the fast increase in food supply chain sustainability, quality control and other food monitoring commodities have gained a lot of interest according to non-destructive testing [Zhang *et al.* (2019)]. Particularly, the pomegranate fruit is highly affected due to climatic changes that contaminate the adjacent fruits if one of the fruit is affected by diseases or pesticides [Bhole and Kumar (2021)].

Recent research has focused highly on computer vision applications for providing agricultural goods to farmers in fruit ripening without any loss in agricultural products. In the past few years, some enhanced automatic techniques like X-ray, bio-chemical sensors and IR spectroscopy intrude interiorly to predict agricultural fruits' shelf life [Fathizadeh *et al.* (2021)]. However, these techniques are highly suffered due to time complexity, cost expensive, and labour consumption [Luo *et al.* (2022)]. Later, the researchers introduced the prediction of shelf life is performed accurately based on physiological loss in weight (PLW), decay loss, shrinkage, gloss index and Firmness of the pome fruit [Sun *et al.* (2017)]. However, the visual attributes together without these parameters affect the consumer's acceptance, leading to direct implications of economic factors. The pome fruit is an important component in inhibiting human health concerns [Miranda *et al.* (2022)]. Few studies have been reported in classifying and predicting the shelf life of pome fruit due to its unstable ripening condition [Kumari *et al.* (2018)].

Recently, artificial intelligence (AI) based techniques have been introduced to face the challenges in the shelf life prediction of pome fruit. The advancements in ML and DL techniques have resulted in handling the pre and post-harvesting to protect the freshness, quality and abandon loss in the fruit varieties [Chaturvedi *et al.* (2019)]. Based on the storage condition, physiological operations like respiration, senescence, and ripening can highly affect the shelf life and quality of the fruits [Tiwari (2019)]. In addition, fruit ripening leads to multiple metabolic approaches like climatic and non-climatic factors [Jha *et al.* (2012)]. Some ML based techniques have been introduced to classify and predict the shelf life based on week and month-wise, respectively. In [Iorliam *et al.* (2021)], ML based k-nearest neighbour (KNN), logistic regression (LR), and naïve Bayes (NB) approaches are introduced to predict the shelf life based on Firmness, PLW, acidic contents etc. In [Ljubobratović *et al.* (2022)], ML based non-linear LR model is introduced to classify the shelf life prediction in orange fruit under different temperature conditions. In [Owoyemi *et al.* (2022)], the ML-based approach is introduced to identify the maturity prediction in peach fruit. The shrinkage level of the fruit is studied in this research. However, the ML based techniques cannot train with a huge number of images, which leads to time complexity and storage consumption.

Nowadays, DL based approaches have grown a lot of interest in gaining enhanced accuracy in classifying and predicting healthy and unhealthy fruits along with shelf life. In [Stasenko *et al.* (2021)], shelf life and decay prediction in apples based on the DL approach is introduced. In [Suzuki *et al.* (2022)], predicting the shelf life and weight loss in persimmon fruits using the DL approach is emphasized. However, these techniques cannot predict the important parameters of physiological loss in weight (PLW), decay loss, shrinkage, gloss index and Firmness of the agricultural products. Hence, in this research, a novel DL based technique is introduced to classify the healthy and unhealthy fruit along with shelf life prediction under different physiological parameters are proposed.

Motivation and problem formulation: Developing trends in recent techniques enhance the accuracy performance for better predicting shelf life in agricultural products. However, shelf life prediction is one of the most challenging and important tasks due to various health concerns, food supply chain and cost concerns. Many studies have been undertaken related to many fruits except pomegranate fruit. Research on pome fruit is rare due to delayed ripening, climatic change and storage consumption. The pome fruit plays an important role in health concerns and has the leading demand in producing fresh juice, syrup, wine, candy, etc. Well-developed techniques are required to predict the shelf life of healthy and unhealthy pome fruit. To the best of our knowledge, the proposed method provides better performance in predicting the shelf life accurately by considering various physiological parameters such as PLW, decay loss, shrinkage, gloss index and Firmness of the pome fruit. The major objectives of the work are:

- To introduce the classification and prediction of pomegranate fruit using MRI images and a deep learning model.
- To introduce an S-ResNet-152 (Squeeze based ResNet-152) model for classifying the fruit as healthy or unhealthy and Binate Attention U-Capsule Network (Binate Att-UCNet) for predicting the shelf life.
- To determine the shelf life using physiochemical and physiological loss in weight (PLW), Decay Loss, Shrinkage and Firmness features.
- To validate the performance of the proposed model with other existing models using several prediction metrics.

The rest of the research work is sorted as follows: Section 2 is the recent related works based on the shelf life of fruits using various models. Section 3 presents the proposed shelf life prediction of pomegranate fruits, Section 4 is the results and discussions, and the entire work is concluded in Section 5.

2. Related Work

Some of the related works based on shelf life prediction using various models are listed below:

[Bird *et al.* (2022)] determined the fruit quality and detective lemon fruit image classification using GAN based data augmentation techniques. In this method, a convolutional neural network (CNN) was introduced to predict the quality of the fruit. Then, a generative adversarial network (GAN) was introduced for the classification of healthy and unhealthy fruit. In addition, augmentation was also undertaken to enhance the accuracy of CNN. The dataset was collected from a publically available dataset of about 2690 images. In the experimental scenario, an accuracy of 88.75% was attained. However, this method suffered due to failure in detecting the fruit shrinkage from the dataset.

[Albert and Osman (2022)] introduced the interactive DL approach for shelf life prediction in muskmelon fruit. In this method, the k-Determinantal Point Processes (k-DPP) technique was introduced to overcome the complexities that arise in the CNN model. The single channel noise reduction (SCNR) technique was introduced to improve the training model's convergence. In the experimental scenario, an accuracy of 73.9%, precision of

77.4% and recall of 67% were attained. Using this technique weight, humidity, temperature, and zone can be analyzed. However, this method suffered due to failure to detect the gloss index from the particular trained image.

[Torres *et al.* (2020)] defined the real time monitoring approach for estimating the shelf life of fruits and vegetables. This method introduced a multi-linear LR approach to accurately predict the shelf life. Here, some of the physiochemical features like delay, respiratory rates, humidity and gas concentration were analyzed. In the experimental scenario, the weight loss obtained was less than 0.025 in 25 days. However, this method was highly limited due lack of detection of gloss index and shrinkage of the fruit.

[Le *et al.* (2020)] defined the application of spectra foot printing during cold storage and the shelf life of packed sweet cheery. This method used partial least squares (PLS) to accurately estimate the cold storage and shelf life of cherry fruit. Here, the weight loss, respiration rate, Firmness, soluble solid content can be analyzed efficiently. In the experimental scenario, the RMSE of 84% was attained. However, this method cannot be suited for classifying the shelf life of pome fruit.

[Cao *et al.*] determined the shelf life prediction in royal gala apples according to the quality attributes and storage temperature. This method introduced sparse-based principle compound analysis with an artificial neural network (SPCA-ANN) technique to predict the post-harvest shelf life for royal gala apples. It can analyze the acidity level in the fruit. In the experimental scenario, the overall correlation coefficient of 0.99 and mean relative error (MRE) of 0.088 was attained. But this method leads to misclassification and high storage consumption problems.

3. Proposed Methodology

One of the important topics in agriculture and food monitoring is the ripeness of agricultural products and quality assessment using non-destructive analysis. Consumers' demand for pomegranate has increased because of its sweet, color and quantity of antioxidants. But, these fruits are spoiled easily with a less shelf life of 10 to 15 days. Hence, it is essential to enhance the shelf life. Most of the research focused on synthetic chemicals that harm the environment and consumers' health. Hence, biological parameters are used for the prediction of shelf life. Figure 1 represents the entire workflow of the proposed model, which consists of two stages, classification and prediction. These two stages are explained briefly in the following sections.

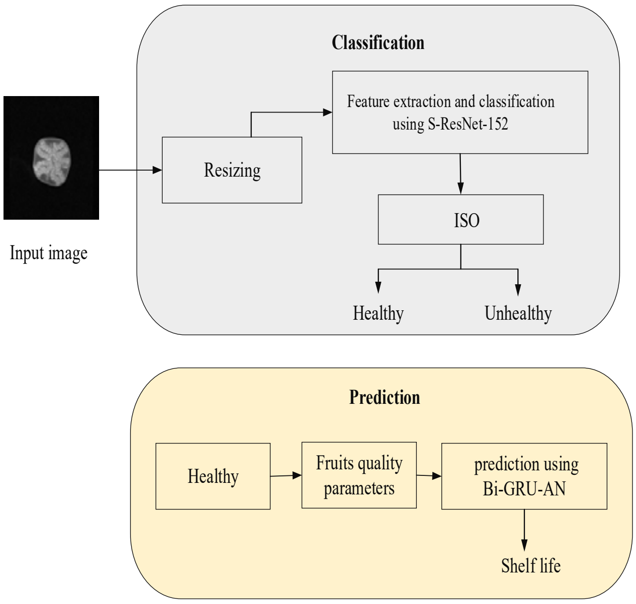

Fig. 1. Workflow of the proposed model

The following analysis is carried out to evaluate the physiochemical parameters needed for the experimentation.

- ***TSS:*** It is one of the essential parameters to determine the quality of fruits. It is the number of soluble minerals and sugar present in pomegranate fruits. Generally, it is obtained from evaluating the fruit's degree Brix. It is determined by using a hand refractometer. It defines 10 to 20% of the weight of the fresh fruits and increases when they mature to produce a less acidic, sweet fruit.
- ***Loss_weight:*** It is identified using weighting the pomegranates at the beginning of the experimentation for every interval with the electronic balance. Loss_weight is periodically computed, and it is the ratio of percentage loss_weight based on the original mass.

- ***pH:*** The pH value of pomegranate fruits is identified by inserting the calibrated pH meter into the pomegranate paste obtained after the blending process, and the readings are noted.
- ***Acidity:*** The acidity of the fruits is identified after the blending process, a certain quantity of juice is filtered by filtering paper. The acidity is determined using

$$Acidity = \frac{vol \times M \times F \times 100}{volume\ of\ \ pomegranate\ \ juice}$$

where vol is the volume of 0.1 N sodium hydroxide (N_aOH), M and F are the N_aOH 's molarity and factor of acid.

- ***Firmness:*** It is used to enhance the storability capacity and induce high resistance to fruit damage. It is the measure of texture property. It is the high penetrating force (N) obtained on the tissue breakage by the probe. The force obtained at the standard probe's penetration up to some height (cm) is the Firmness, measured by a penetrometer. Nearly six measurements are made on every fruit at various locations for computing the Firmness.

3.1 *Pre-processing*

Initially, the input pomegranate fruits have different dimensions, hence it is hard to train deep learning (DL). Therefore, image resizing is essential, and it is the process of scaling input images. In this work, the input images are scaled to the dimension of 256x256.

3.2 *Feature extraction and classification*

After the images are resized, the hybrid model S-ResNet-152 carries out the feature extraction and classification processes. Initially, the SqueezeNet model initiates with a convolutional layer, eight fire layers and ends with the convolutional layer. In this structure, the final convolutional layer is replaced by SqueezeNet, and the ResNet-152 is added to the structure, as shown in Figure 2. The structure of SqueezeNet depends on three models for minimizing the number of parameters in the network. These models replace 3x3 filter with 1x1 filter, minimizing the number of input channels to 3x3 filters and evaluating downsampling in the network. It permits the convolutional layers to obtain better activation maps. This network relies on various "Fire layers" comprising "Fire modules".

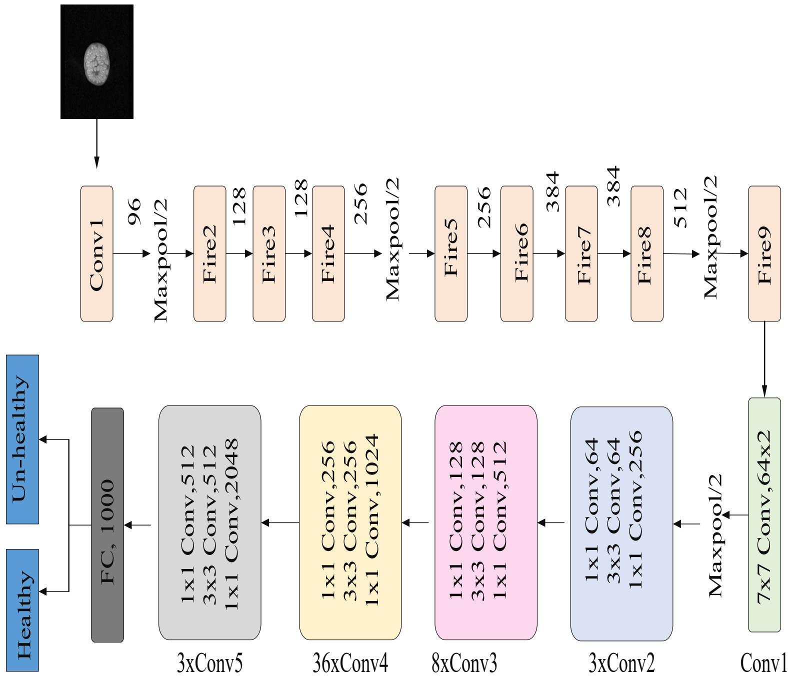

Fig. 2. Architecture of S-ResNet-152

This module has squeezed the convolutional layer and fed it to the expand layer, which has both 1x1 and 3x3 convolutional filters. The fire layer has squeezed and expanded layers between the convolutional layers. The squeeze layer has a filter size of 1x1, and the expand layer has a filter size of 1x1 and 3x3. The operation Squeeze is used to compress the depth and expand it improves the depth by maintaining the same feature size. Let C_h and f_m are the channels and feature maps of the squeeze operation with the kernel k and the output layer $f(z)$ given as:

$$f(z) = \sum_{F_m=1}^{f_m} \sum_{C=1}^{c} k_C^f y_C^{f_m} \quad (1)$$

To improve the accuracy in classification, the ResNet-152 model is integrated with the SqueezeNet model. The ResNet-152 has an architecture named residual learning unit with 152 layers. This model is used for reducing the vanishing problem, and a short-cut connection is given to the input a , and various convolutional layers follow it.

$$f(a) = R(a, W) + a \quad (2)$$

where $R(a)$ is the residual mapping to the identity, $f(a)$ and W are the output and weight of residual blocks.

The identity short-cuts are provided to the input and output with the same measurements and are given as:

$$f(a) = R(a, W_i) + a \quad (3)$$

When there is a difference in measurements, the short-cuts find mapping and zero entities padded with the improved measurements. Then, the projection short-cut is provided for matching the dimension, and it is given as:

$$f(a) = R(a, W_i) + W_s a \quad (4)$$

where W_s is the additional variable.

Here, the cross entropy is used as the loss function, and it is expressed as:

$$L_{CE} = -\sum_{j=1}^{N} p^{(j)} \log q^{(j)} \quad (5)$$

where N is the total classes, $p^{(j)}$ and $q^{(j)}$ are the true and predicted labels at the j^{th} class.

3.2.1.Weight selection using ISO

Hyperparameters play a major role in DL models, and optimizing these parameters are essential since it improves the training process. To achieve better training and improve the performance of the DL model, the metaheuristic algorithm Improved Sandpiper Optimization (ISO) is introduced in this work. Sandpipers are birds generally seen in the sea, are omnivorous, and eat earthworms, fishes, and reptiles. They use bream crumps for hunting fish and are habited in colonies. They utilize their intelligence to identify and attack their prey. The major thing about sandpipers is their migration and attacking characteristics. The mathematical modelling of these two characteristics in the sandpiper optimization algorithm (SOA) [Kaur *et al.* (2020)] is described below:

Migration characteristics: It is the exploration stage, and during this migration process, the sandpipers move into the group. In the migration process, the set of sandpipers swings from one place to another. In this phase, the sandpipers must undergo the three strategies:

Avoiding collision: The parameter C_d is utilized to calculate the position of the new search agent for overcoming the collision among other sandpipers.

$$\vec{C}_{sa} = C_d \times \vec{P}_{sa}(y) \quad (6)$$

where $\vec{C}_{sa}$ is the search agent's position, which doesn't collide with each other, $\vec{P}_{sa}(y)$ is the present search agent's position at the iteration y and C_d is the movement of the search agent in the searching space.

$$C_d = D_g - (y \times (D_g / \max\_iter)) \quad (7)$$

where D_g is the adjusting frequency, and it is used for managing C_d

Converge to the direction of the best neighbour: after avoiding the collision, the search agents converge to the best neighbouring direction. It is represented as:

$$\vec{M}_{sa} = C_r \times (\vec{P}_b(y) - \vec{P}_{sa}(y)) \quad (8)$$

where $\vec{M}_{sa}$ is the place of search agent to the best search agent $\vec{P}_b$. C_r is the random parameter and is used to balance the exploration, and it is represented as:

$$C_r = 0.5 \times r_n \quad (9)$$

where r_n is the random number, and it ranges from 0 to 1.

Update by means of the best search agent: The sandpipers update the position with respect to the best search agent. It is expressed as:

$$\vec{D}_{sa} = \vec{C}_{sa} + \vec{M}_{sa} \quad (10)$$

$\vec{D}_{sa}$ is the distance between the sandpiper and best search agent.

Attacking characteristics: The search agents can change the angle of attack and speed during the migration process. The wings are used for improving the height, and the search agents make the spiral characteristics during the exploitation (attacking). This characteristic is described in the 3-D plane, and it is represented as:

$$X' = \mathrm{Rad} \times \sin(k) \qquad (11)$$

$$Y' = \mathrm{Rad} \times \cos(k) \qquad (12)$$

$$Z' = \mathrm{Rad} \times k \qquad (13)$$

$$r_n = w \times \exp(v) \qquad (14)$$

where Rad is the radius of every turn of the spiral and k is the parameter which ranges between 0 and 2π. w and v are the fixed variables used to define the spiral shape. Finally, the updated position of the sandpiper is calculated as follows:

$$\vec{P}_{sa}(y) = (\vec{D}_{sa} \times (X' + Y' + Z')) \times \vec{P}_b(y) \qquad (15)$$

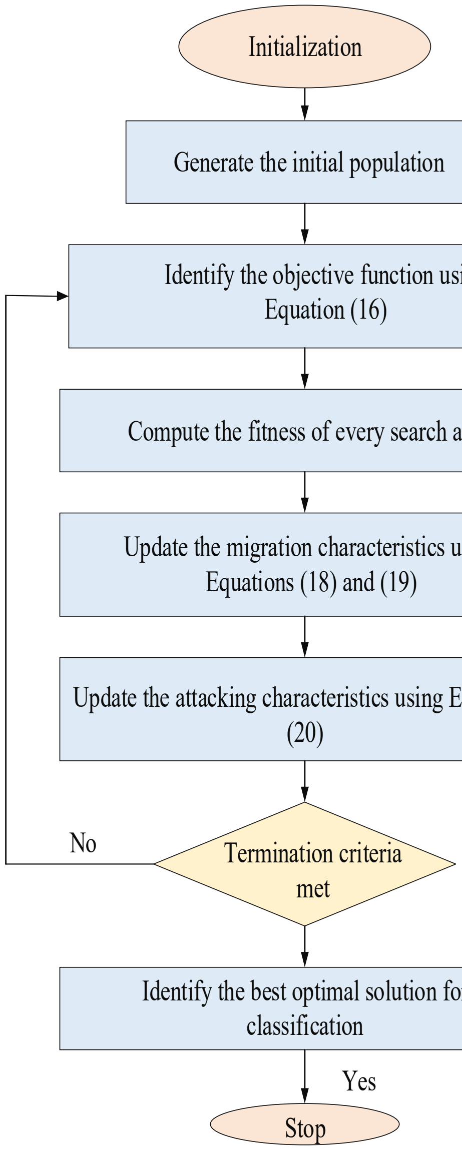

Fig. 3. Flowchart of the ISO algorithm

The standard optimization SOA is the new optimization that can be utilized in various fields to solve optimization issues. The position of sandpipers in the solution space is distributed randomly. This may minimize the convergence accuracy and be trapped by local optima. Hence, an adaptive learning factor (ALF) is used to overcome this problem. The fitness function is computed using the following expression:

$$Fitness = W_{acc} \times accuracy + W_b \times \frac{1}{N} \quad (16)$$

where W_{acc} is the accuracy weight, W_b is the weight of the features involved for classification and N is the total number of samples.

The ALF of the sandpiper at t^{th} iteration is expressed as:

$$b^t = \frac{1}{1+\exp(-u)} \quad (17)$$

The value of u ranges from 0 to 2.

Hence, the updated positions of avoiding collision in Equation (6) converge to the direction of the best neighbour in Equation (8). The updated position of the sandpiper in Equation (15) is expressed as follows:

$$\vec{C}_{sa} = b^t \times C_d \times \vec{P}_{sa}(y) \quad (18)$$

$$\vec{M}_{sa} = b^t \times C_r \times (\vec{P}_b(y) - \vec{P}_{sa}(y)) \quad (19)$$

$$\vec{P}_{sa}(y) = b^t \times (\vec{D}_{sa} \times (X' + Y' + Z')) \times \vec{P}_b(y) \quad (20)$$

Hence, these improved Equations improve the classification performance by considering the fitness function using Equation (16). Figure 3 shows the flowchart of the ISO algorithm.

3.3 *Prediction using Bi-GRU-AN*

Healthy pomegranate images are considered for the prediction of shelf life prediction. For predicting the shelf life, the parameters like physiochemical and physiological loss in weight (PLW) and Firmness are considered for determining the fruit quality. The hybrid deep learning model bidirectional gated auto network (Bi-GRU-AN) is used for the prediction. The architecture of Bi-GRU-AN is given in Figure 4, which has layers like the input layer, Bi-GRU, AN layer and output layer. The features like physiochemical and physiological loss in weight (PLW) and Firmness with the healthy images are given as input to the input layer. Every block in Bi-GRU has a cell used for storing the information. The blocks are made up of an update gate and a reset gate. The update gate verifies the previous memory, and the reset gate combines the new input and previous memory. There are two GRU blocks in Bi-GRU, and the gates in Bi-GRU are used for storing information in forward and backward directions. Further, it uses both past and future contexts in the sequence, and it is expressed as:

$$h_t = \left[\vec{h}_t, \overleftarrow{h}_t\right] \quad (21)$$

where $\vec{h}_t$ and $\overleftarrow{h}_t$ are the forward and backward blocks.

The final output layer at the time t is given as:

$$z_t = \sigma(W_z h_t + b_z) \quad (22)$$

where σ is the activation function, W_z and b_z are the weight and bias factors.

$$y_t = \sigma_h(W_z u_t + U_y h_{t-1} + b_y) \quad (23)$$

$$s_t = \sigma_h(W_s u_t + U_s h_{t-1} + b_s) \quad (24)$$

$$h_t = y_t h_{t-1} + (1 - y_t) \otimes \phi g(W_g u_t + U_g(s_t \otimes h_{t-1}) + b_g \quad (25)$$

where u_t, s_t, z_t and h_t are the input vector, reset gate, update gate and output vector with respect to bias and weighs. W and U are the weighted variables. $\otimes$ is the Hadamard product, σ_h and ϕg are the sigmoid and hyperbolic tangent.

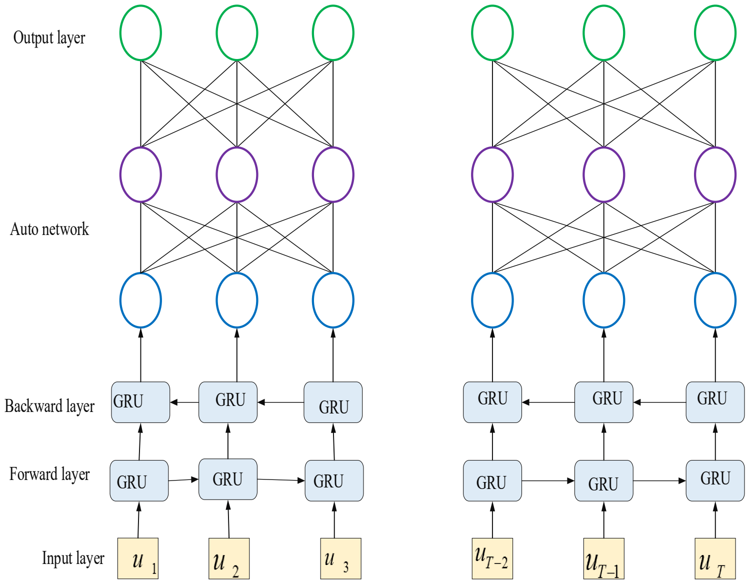

Fig. 4. Architecture of Bi-GRU-AN

An Autoencoder network (AN) is a multi-layer network that exploits the backpropagation (BP) based on the loss function in which the input and output are the same. The AN model has three major elements like Encoder and Decoder. The encoder compresses the input and generates the latent pattern, and the encoder is used for reconstructing the input by latent pattern. The encoding and decoding procedures are represented as follows:

$$q_j = f(w_q y_j + b_t) \qquad (26)$$

$$y_j = g(w_y q_j + b_t) \qquad (27)$$

where $f()$ and $g()$ are the sigmoid function, w and b are the weight and bias factors. The loss function utilized for training the model is given as follows:

$$Loss = \frac{1}{2n} \| x_k - y_k \|^2 \qquad (28)$$

where x_k and y_k are the observed and predicted values and n is the total number of samples.

4. Results and Discussion

This section discusses the result analysis of the shelf life prediction using the proposed model. The entire implementation is carried out on the Python platform. Further, the performance of the proposed model is compared with other models based on the square of correlation coefficient (R^2), root mean square error of calibration (RMSEC), and root mean square error of validation (RMSEV).

4.1 *Dataset details*

A total of 199 fruits were collected from Shej Babulgaon, Mohol, Tal and District Solapur from August to November. To predict the shelf life of the fruits, the parameters like initial weight, final weight, TSS, Ph, acidity and Firmness are collected from the National Research Center on Pomegranate (NRCP), Solapur, Maharashtra, India. MRI modality is used for scanning pomegranate fruits. Some of the MRI images obtained from the laboratory are given in Figure 5.

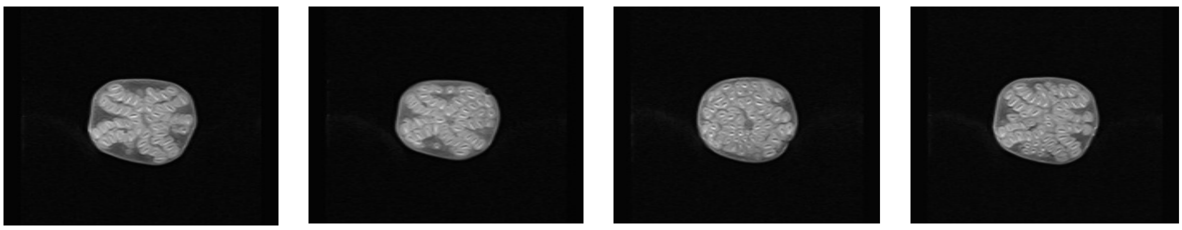

Fig. 5. Sample MRI images obtained from the laboratory

4.2 *Performance Measures*

For computing, the performance metrics of the classification performances like accuracy, sensitivity, precision, F1 score and specificity are computed. Then, the prediction measures like R^2, RMSEC and RMSEV are computed.

Accuracy: It is the proportion of correctly classified samples to the entire samples, and it is expressed as:

$$A = \frac{T_p + T_n}{T_p + T_n + F_p + F_n} \qquad (29)$$

Sensitivity: It is the number of total positive predictions to the number of entire positive samples. It is expressed as:

$$Se = \frac{T_p}{T_p + F_n} \qquad (30)$$

Specificity: It is the ratio of negative cases that are predicted as negative, and it is expressed as:

$$Sp = \frac{T_n}{T_n + F_p} \qquad (31)$$

Precision: It is also called positive predictive value (PPV), and it is the ratio of positive predictions that are actually predicted as positive cases. It is expressed as:

$$P = \frac{T_p}{T_p + F_p} \qquad (32)$$

F1 score: It is the harmonic mean among Sp and P , and it is expressed as:

$$F1 - score = \frac{2T_p}{2T_p + F_p + F_n} \qquad (33)$$

R^2: The ratio of the difference in dependent parameters is predicted from the independent parameter. It is expressed as:

$$r = \frac{\sum_{i=1}^{m}\left(\hat{z}_i - z_i\right)^2}{\sum_{i=1}^{m}\left(\hat{z}_i - z_n\right)^2} \qquad (34)$$

RMSEC: It is the square root of the mean squared variation between the actual and predicted features, which is obtained by calibration. It is expressed as:

$$RMSEC = \sqrt{\frac{1}{n_c}\sum_{i=1}^{n_c}\left(\hat{z}_i - z_i\right)^2} \qquad (35)$$

RMSEV: It is used for obtaining the variation between the actual and predicted features in the validation process.

$$RMSEV = \sqrt{\frac{1}{n_v}\sum_{i=1}^{n_v}\left(\hat{z}_i - z_i\right)^2} \qquad (36)$$

where $\hat{z}_i$ is the predicted sample at the observation of i , z_n and z_i are the actual samples at the calibration and validation set. n, n_c and n_v are the number of samples.

4.3 *Performance comparison*

The performance of the proposed model is compared with the existing models in terms of classification and prediction.

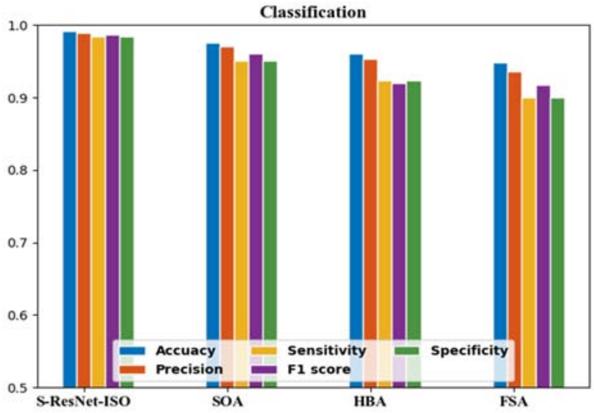

Fig. 6. Comparison of classification performance

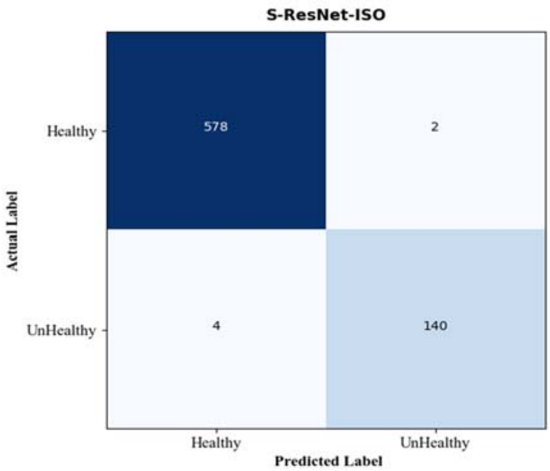

Fig. 7. Confusion matrix of the proposed S-ResNet-ISO

Figure 6 represents the comparison of the classification performance of the various models. The measures like accuracy, sensitivity, precision, F1 score and specificity are computed for the methods like SOA, HBA (honey badger algorithm) and FSA (Flamingo search algorithm) and the proposed S-ResNet-ISO. The accuracy of the proposed S-ResNet-ISO, SOA, HBA and FSA are 0.991, 0.975, 0.961 and 0.948, respectively. Further, the precision value achieved by the proposed S-ResNet-ISO is 0.989, which is 1.92 %, 3.74%, and 5.46% better than SOA, HBA and FSA optimization techniques. Similarly, the sensitivity, F1 score and specificity values achieved by the proposed S-ResNet-ISO model are higher than other approaches. This performance is achieved due to the better weight selection by ISO. While other optimization techniques suffered due to slow convergence; hence these models achieved poor results.

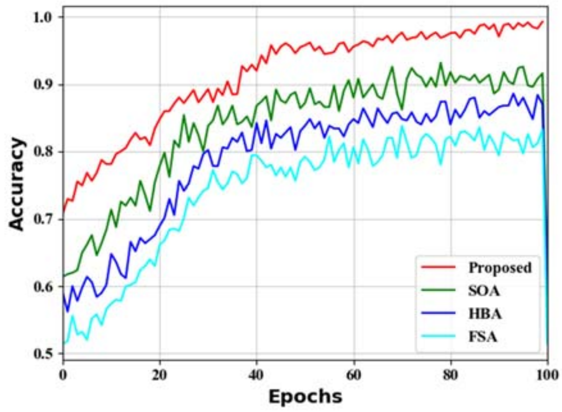

(a)

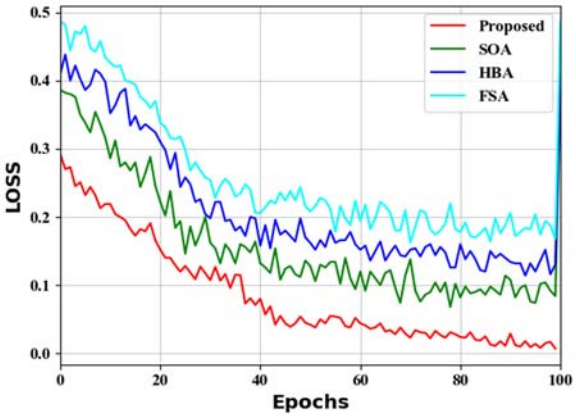

(b)

Fig. 8. Performance of (a) Accuracy (b) Loss

Figure 7 represents the confusion matrix of the proposed S-ResNet-ISO model. The tested outcomes are given in the confusion matrix form, which measures the efficiency of the proposed S-ResNet-ISO model. This matrix has more details regarding the accuracy and training performance. The actual class is in a row, and the prediction class is in a column. Here, the confusion matrix is given for two classes, healthy and unhealthy. Every element of the matrix compares the true label and the predicted label. The Figure shows that the 578 images are predicted as healthy out of 580 images.

Figure 8 represents the performance of accuracy and loss curves of the proposed S-ResNet-ISO, SOA, HBA and FSA models for the epoch values of 100. In Figure 8 (a), the accuracy is also increased when the epoch value is increased. When the epoch value is 100, the accuracy is 0.998 for the S-ResNet-ISO model. Similarly, in Figure 8 (b), the loss is decreased when the epoch value is increased. Particularly, when the epoch is 100, the loss is very less for all the models.

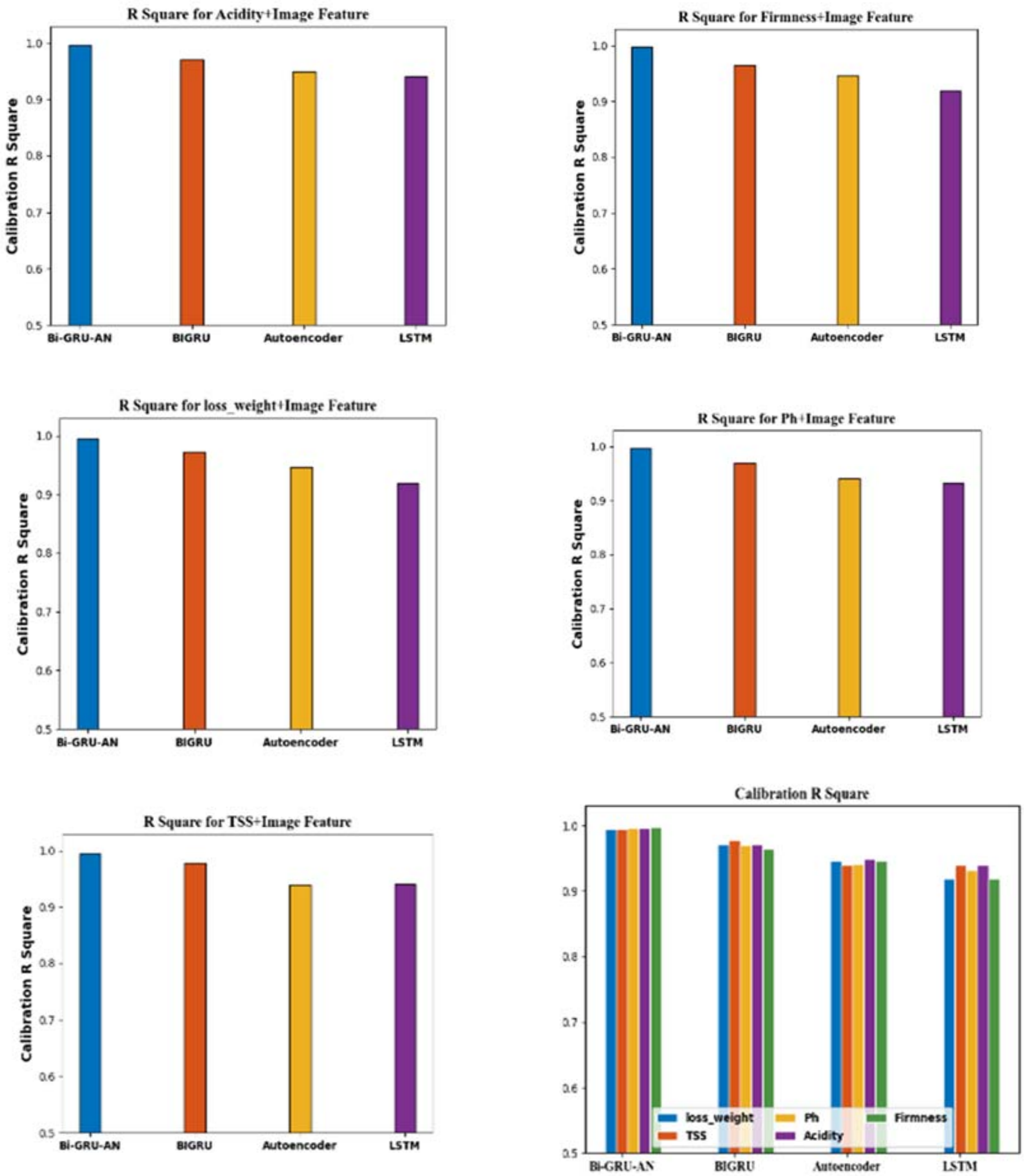

Fig. 9. Performance of Calibration R^2 of various models

Figure 9 represents the performance of Calibration R^2 of various models like LSTM, autoencoder, Bi-GRU and the proposed Bi-GRU-AN models. Here, the prediction is carried out by physiochemical parameters like acidity, Firmness, pH, loss_weight and TSS with the features obtained from the image. When considering the acidity parameter, the Calibration R^2 value of the proposed Bi-GRU-AN model is 0.9962, Bi-GRU is 0.9713, autoencoder is 0.9494, and LSTM is 0.9398, respectively. When comparing the overall performance of Calibration R^2, for the parameter firmness, the value of Calibration R^2 is high. For the firmness parameter, the Calibration R^2 value of the proposed Bi-GRU-AN model is 0.9973, Bi-GRU is 0.9642, autoencoder is 0.9463, and LSTM is 0.9183, respectively. Hence, it is proved that the shelf life prediction relies mainly on the firmness parameter.

Figure 10 represents the performance of RMSEC of various models like LSTM, autoencoder, Bi-GRU and the proposed Bi-GRU-AN. The RMSEC value should be very less for a better classification model. In this comparison, The RMSEC values of loss_weight with image features of the LSTM, autoencoder, Bi-GRU and the proposed Bi-GRU-AN models are 0.6619, 0.5370, 0.3923 and 0.0151. Further, when comparing the overall performance, the proposed prediction model Bi-GRU-AN achieved better RMSEC values in all the parameters. For the firmness parameter, the RMSEC value of the proposed prediction model Bi-GRU-AN achieved less error of 0.0114. Finally, it is concluded that the shelf life prediction mainly depends on the firmness parameter.

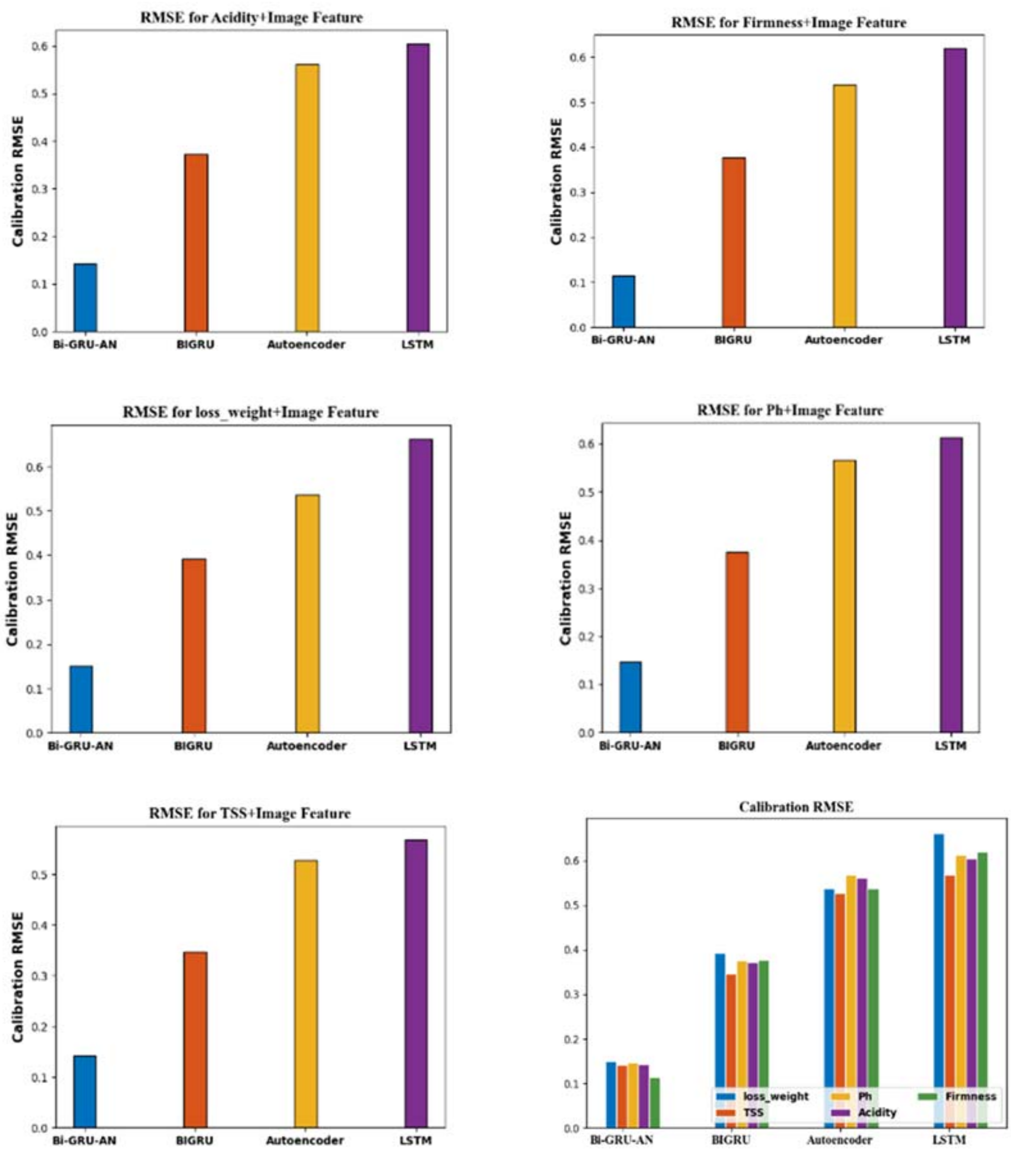

Fig. 10. Performance comparison of RMSEC

Figure 11 shows the performance of validation R^2 of various models like LSTM, autoencoder, Bi-GRU and the proposed Bi-GRU-AN. The graphical representation shows that the proposed model achieved a better correlation coefficient for all the features. The validation R^2 value achieved by the proposed Bi-GRU-AN is 0.9963, 0.9978, 0.9958, 0.9963 and 0.9965 for acidity, Firmness, pH, loss_weight and TSS with the image features. From this observation, it is proved that the shelf life prediction of the fruits is mainly based on Firmness compared to other parameters.

Figure 12 represents the performance of RMSEV of various models like LSTM, autoencoder, Bi-GRU and the proposed Bi-GRU-AN. The better model performance must have low values of RMSEV; for the TSS parameter, the RMSEV values obtained by the LSTM, autoencoder, Bi-GRU and the proposed Bi-GRU-AN are 0.6149, 0.5042, 0.3803 and 0.0147 respectively. Then, for the firmness parameter, the RMSEV values obtained by the LSTM, autoencoder, Bi-GRU and the proposed Bi-GRU-AN are 0.6186, 0.5480, 0.3765 and 0.0116, respectively. The proposed model achieved better results due to the hybrid structure of Bi-GRU and AN. The existing models achieved poor results due to overfitting issues and have a complex structure.

Figure 13 represents the actual and prediction plot of the shelf life prediction of the pomegranate fruits. This plot is used to find whether the method is satisfactory and provides the agreement between the original and the predicted data. The prediction of fresh fruit, one-month to three month fruits with respect to acidity and firmness parameters are given. Here, the actual values are given in a straight line and predicted values are given in dots. In this plot, the RMSE values obtained by the proposed model for the calibration and validation chart are 0.0114 and 0.0116, respectively.

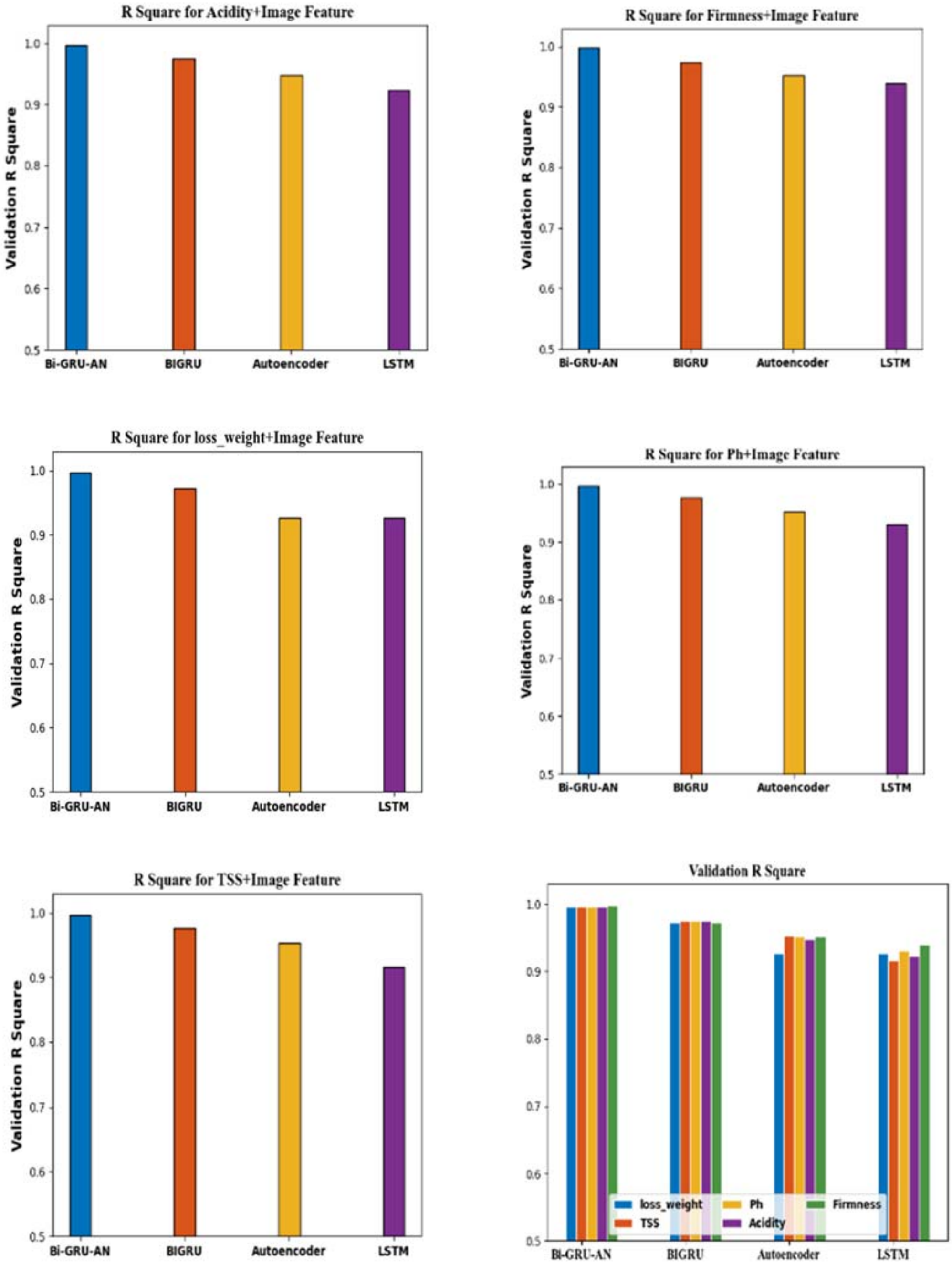

Fig. 11. Performance of validation R^2 of various models

Figure 14 shows the actual and prediction plot of the shelf life prediction Calibration chart and validation chart of loss_weight, pH and TSS. Here, the prediction is taken for the fresh fruits and the fruits obtained from the three month prediction. Here. In Figure 14 (a), R2 and RMSE achieved for the loss_weight are 0.9957 and 0.0151 for calibration and 0.9963 and 0.0143 for validation. Further, in Figure 14 (b), shelf life predicted based on pH values of R2 and RMSE are 0.9961and 0.0146 for calibration and 0.9958 and 0.0150 for validation. Similarly, in Figure 14 (c), the R2 and RMSE obtained for the TSS are 0.9956 and 0.0142 (calibration) and 0.9965 and 0.0147 (validation) achieved by the proposed model.

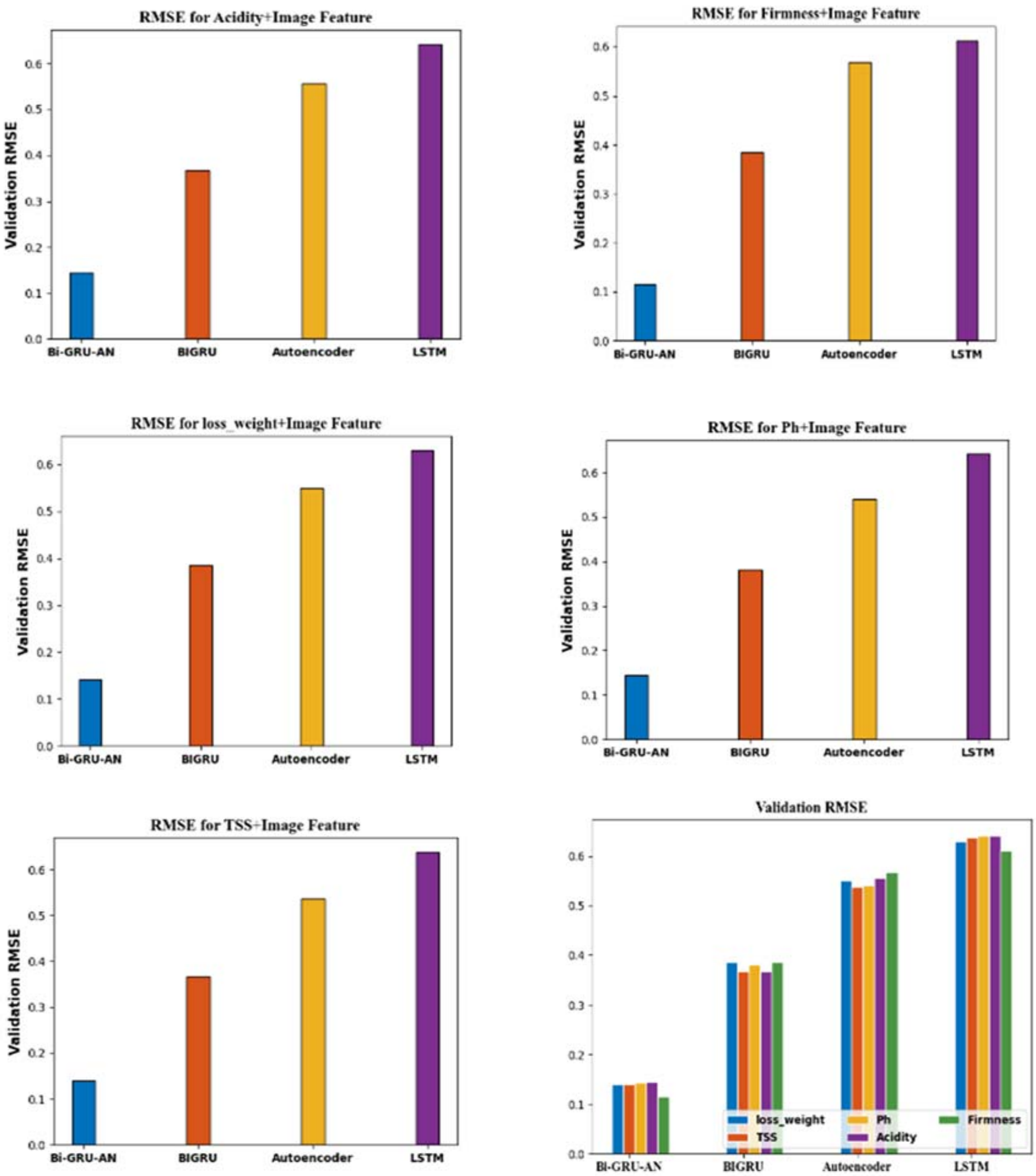

Fig. 12. Performance comparison of RMSEV

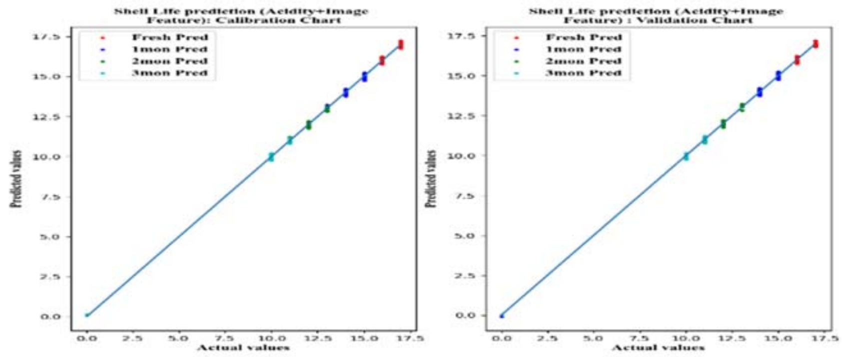

(a)

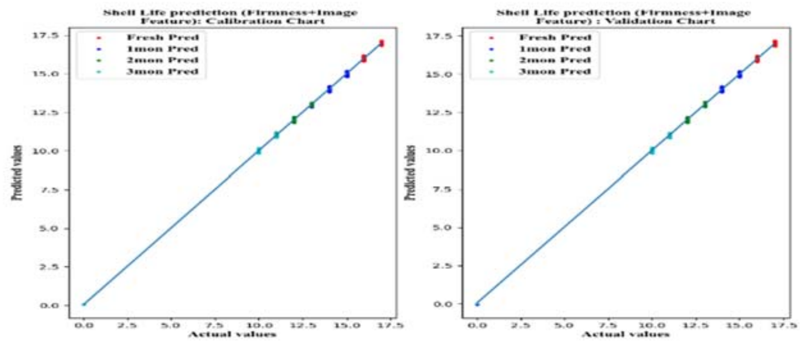

(b)

Fig. 13. Actual and prediction plot of shelf life prediction Calibration chart and validation chart (a) acidity (b) firmness

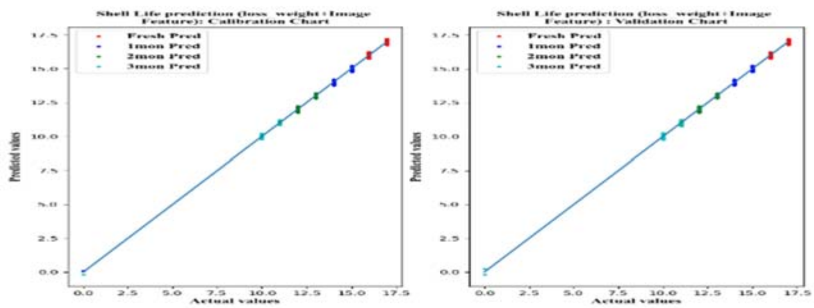

(a)

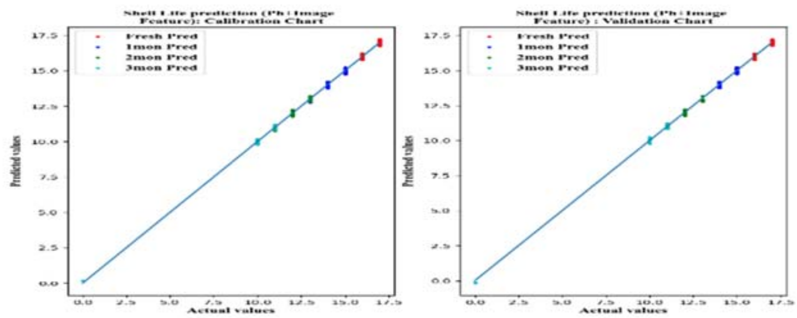

(b)

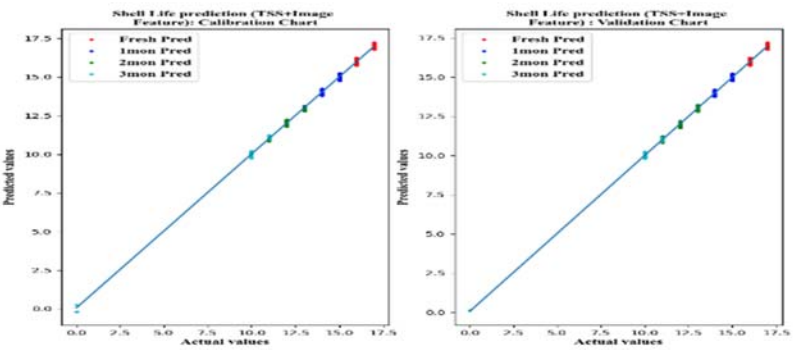

(c)

Fig. 14. Actual and prediction plot of shelf life prediction Calibration chart and validation chart (a) loss_weight (b) pH (c) TSS

5. Conclusion

In this work, two major processes, classification and prediction, are carried out. The following processes are performed to classify the fruits as healthy and unhealthy. The MRI pomegranate fruits are collected from the NRCP research center for experimentation. Initially, the DL model S-ResNet is used to classify healthy and unhealthy images. Then, for the further prediction process, healthy fruits are considered, and the BI-GRU-AN model carries it out. Physiological parameters like acidity, Firmness, pH, loss_weight and TSS are considered in the prediction process. The classification performances are computed for the proposed and existing models, and the proposed model achieved better accuracy and precision of 0.991 and 0.989, respectively. Then, the prediction measures like R^2, RMSEC and RMSEV are computed. Here, the RMSEC and RMSEV values are very low, and the R2 value is high for the proposed model compared to other DL models. The experimental observation proved that the shelf life prediction is mainly based on the parameters Firmness compared to other parameters.

Conflict of Interest Statement:

The author(s) declare(s) that there is no conflict of interest.

References

[1] Felicia W. X. L.; Rovina K.; Nur'Aqilah M. N.; Vonnie J. M.; Erna K. H.; Misson M.; Halid N. F. A. (2022): Recent Advancements of Polysaccharides to Enhance Quality and Delay Ripening of Fresh Produce: A Review, Polymers, **14**(7), p.1341.

[2] Althaus B.; Blanke M. (2021): Development of a Freshness Index for Fruit Quality Assessment—Using Bell Pepper as a Case Study, Horticulturae, **7**(10), p.405.

[3] Zhang R.; Lan, W.; Ding J.; Ahmed S.; Qin W.; He L.; Liu Y. (2019): Effect of PLA/PBAT antibacterial film on storage quality of passion fruit during the shelf-life, Molecules, **24**(18), 3378.

[4] Bhole V.; Kumar A. (2021): A transfer learning-based approach to predict the shelf life of fruit, Inteligencia Artificial, **24**(67), pp.102-120.

[5] Fathizadeh Z.; Aboonajmi M.; Hassan-Beygi S. R. (2021): Classification of apples based on the shelf life using ANN and data fusion, Food Analytical Methods, **14**(4), pp.706-718.

[6] Luo L.; Sun W.; Cao S.; Liu J.; Kong F. (2022): Facility tomato picking system based on shelf life prediction and fruit maturity discrimination, In 2022 IEEE Asia-Pacific Conference on Image Processing, Electronics and Computers (IPEC), pp. 490-492. IEEE.

[7] Sun K.; Li Y.; Peng J.; Tu K.; Pan L. (2017): Surface gloss evaluation of apples based on computer vision and support vector machine method, Food Analytical Methods, 10(8), pp. 2800-2806.

[8] Miranda M.; Marilene De Mori M. R.; Spricigo P. C.; Pilon L.; Mitsuyuki M. C.; Correa D. S.; Ferreira M. D. (2022): Carnauba wax nanoemulsion applied as an edible coating on fresh tomato for postharvest quality evaluation, Heliyon, **8**(7), p.e09803.

[9] Kumari P.; Ahmad M. F.; Mir H. (2018): Non-destructive quality evaluation by sensing maturity and ripening of fruits and vegetables, Journal of Postharvest Technology, **6**(2), pp.84-89.

[10] Chaturvedi K.; Sharma N.; Yadav S. K. (2019): Composite edible coatings from commercial pectin, corn flour and beetroot powder minimize post-harvest decay, reduces ripening and improves sensory liking of tomatoes, International journal of biological macromolecules, 133, pp.284-293.

[11] Tiwari A. (2019): Nondestructive Methods for Size Determination of Fruits and Vegetables, In Processing of Fruits and Vegetables, pp. 203-221. Apple Academic Press.

[12] Jha S. N.; Rai D. R.; Shrama R. (2012): Physico-chemical quality parameters and overall quality index of apple during storage, Journal of food Science and technology, 49(5), pp.594-600.

[13] Iorliam I. B.; Ikyo B. A.; Iorliam A.; Okube E. O.; Kwaghtyo K. D.; Shehu Y. I. (2021): Application of Machine Learning Techniques for Okra Shelf Life Prediction, Journal of Data Analysis and Information Processing, **9**(3), pp.136-150.

[14] Ljubobratović D.; Vuković M.; Brkić Bakarić M.; Jemrić T.; Matetić M. (2022): Assessment of Various Machine Learning Models for Peach Maturity Prediction Using Non-Destructive Sensor Data, Sensors, **22**(15), p.5791.

[15] Owoyemi A.; Porat R.; Lichter A.; Doron-Faigenboim A.; Jovani O.; Koenigstein N; Salzer Y. (2022): Evaluation of the Storage Performance of 'Valencia'Oranges and Generation of Shelf-Life Prediction Models, Horticulturae, **8**(7), p.570.

[16] Stasenko N.; Savinov M.; Burlutskiy V.; Pukalchik M.; Somov A. (2021): Deep Learning for Postharvest Decay Prediction in Apples, In IECON 2021–47th Annual Conference of the IEEE Industrial Electronics Society, pp. 1-6. IEEE.

[17] Suzuki M.; Masuda K.; Asakuma H.; Takeshita K.; Baba K.; Kubo Y.; Ushijima K.; Uchida S.; Akagi T. (2022): Deep Learning Predicts Rapid Over-softening and Shelf Life in Persimmon Fruits, The Horticulture Journal, pp.UTD-323.

[18] Bird J. J.; Barnes C. M.; Manso L. J.; Ekárt A.; Faria D. R. (2022): Fruit quality and defect image classification with conditional GAN data augmentation, Scientia Horticulturae, 293, p.110684.
[19] Albert-Weiss D.; Osman A. (2022): Interactive Deep Learning for Shelf Life Prediction of Muskmelons Based on an Active Learning Approach, Sensors, **22**(2), p.414.
[20] Torres-Sanchez R.; Martínez-Zafra M. T.; Castillejo N.; Guillamon-Frutos A.; Artes-Hernandez F. (2020): Real-time monitoring system for shelf life estimation of fruit and vegetables, Sensors, 20(7), p.1860.
[21] Le Nguyen L. P.; Visy A.; Baranyai L.; Friedrich L.; Mahajan P. V. (2020): Application of hue spectra fingerprinting during cold storage and shelf-life of packaged sweet cherry, Journal of Food Measurement and Characterization, **14**(5), pp.2689-2702.
[22] Cao M.; Wang D.; Qiu L.; Ren X.; Ma H. (2021): Shelf Life Prediction of 'Royal Gala'Apples Based on Quality Attributes and Storage Temperature, pp. 343-355.
[23] Kaur A.; Jain S.; Goel S. (2020): Sandpiper optimization algorithm: a novel approach for solving real-life engineering problems, Applied Intelligence, **50**(2), pp.582-619.
[24] Özdemir K. S.; Gökmen V. (2017): Extending the shelf-life of pomegranate arils with chitosan-ascorbic acid coating, LWT-food science and technology, 76, pp.172-180.
[25] Dak M.; Sagar V. R.; Jha S. K. (2014): Shelf-life and kinetics of quality change of dried pomegranate arils in flexible packaging, Food Packaging and Shelf Life, **2**(1), pp.1-6.

Authors Profile

Surekha V. Yakatpure obtained B.E. degree in the department of electronics and telecommunications at JNEC, Marathwada University, Aurangabad. Also, she obtained M.E. degree in the department of electronics and telecommunication at KIT, Solapur University, Kolhapur. Currently, she is pursuing PhD from VTU in Belagavi, Karnataka. Her areas of specialization are image processing, pattern recognition, machine learning, and signal processing. She has 23 years of teaching experience. Presently, she is working as an assistant professor in the department of electronics and telecommunications at A G Patil Institute of Technology, Solapur, India. Honours and Awarded with Fellowship to IEI Calcutta. Life member to ISTE. BOS member at Solapur University.

Dr. Krupa R Rasane is currently working as a Professor & Head of the department of Electronics and Communications at Jain College of Engineering Belgavi, India. Honours and awards include Outstanding Small Branch Counsellor Award IEEE Bangalore Section 2020. Best IEEE Researcher Award in IEEE Bangalore Section Membership to bodies are IEEE USA, Senior IEEE Member Computer Society of India. Her research interest includes Automation and Control Systems Areas and subject expertise include embedded system, Image compression using VLSI, IOT and Network Cybersecurity.

Dr. K. Dhinesh Babu obtained B.Sc (Agri.) degree from Faculty of Agriculture, Annamalai University in 1995, M.Sc.(Horticulture) from Horticulture College & Research Institute, Tamil Nadu Agricultural University, Coimbatore in 1998 and Ph.D (Horticulture) from College of Horticulture, Kerala Agricultural University, Thrissur, Kerala in 2005.